ACCEPTED MANUSCRIPT • OPEN ACCESS

On how fast ions enhance the regulation of drift wave turbulence by zonal flows

To cite this article before publication: Gyungjin Choi *et al* 2023 *Nucl. Fusion* in press https://doi.org/10.1088/1741-4326/ad0f5f

On how fast ions enhance the regulation of drift wave turbulence by zonal flows

G.J. Choi[1], **P.H. Diamond**[2*], **and T.S. Hahm**[1†]

[1] Nuclear Research Institute for Future Technology and Policy, Seoul National University, Seoul 08826, Korea

[2] Department of Astronomy and Astrophysics and Department of Physics, University of California San Diego, La Jolla, CA 92093, USA

E-mail: *`pdiamond@ucsd.edu`, †`tshahm@snu.ac.kr`

Revised November 7, 2023

Abstract. This paper presents a mechanism for enhanced regulation of drift wave turbulence by zonal flows in the presence of a fast ion population. It demonstrates that dilution effects due to the energetic particles have a far-reaching impact on all aspects of the nonlinear dynamics. The modulational growth of zonal flow shear and the corresponding evolution of drift wave energy are calculated with dilution effects. The coupled zonal flow growth and drift wave energy equations are reduced to a predator-prey model. This is solved for the fixed points, which represents the various states of the system. Results display a strong dependence on dilution, which leads to greatly reduced levels of saturated turbulence and transport. Implications for the FIRE mode plasma of KSTAR are discussed in detail. This model is perhaps the simplest dynamical one which captures the beneficial effects of energetic particles on confinement.

1. Introduction

Energetic particles and their dynamics have long been of interest in magnetic confinement, especially with auxiliary heating. Over time, a conceptual multi-component model of the plasma as a 'thermal' population and an energetic particle (EP) population has arisen. Each component can drive various collective modes, most notably drift-ITG modes (DW) by the thermals [1] and Alfven eigenmodes (AEs) by the EPs [2]. This concept in turn motivated the question of the effect of EPs on confinement and transport, and recently, a rise in intense interest in cross-scale coupling between EP-driven modes (typically AEs) and familiar drift wave turbulence [3–9]. One obvious locus of interaction of EP-scale (high frequency) and thermal scale (low frequency) excitations is via zonal modes (i.e., flows and corrugation) since quadratic self-beats of AEs and DWs can both generate zonal flows [10–15].

A particular instance of improved confinement associated with a significant EP population is the FIRE mode, recently discovered on KSTAR [16]. Here FIRE refers to Fast Ion Regulated Enhancement. FIRE mode is a low-density, hot ion ITB plasma with an L-mode edge. The FIRE plasma is characterized by a centrally peaked fast ion distribution, with a significant charge density relative to the electron density - i.e., $f = Z_f n_{f0}/n_{e0} \sim 0.3$. The EP profile is centrally peaked ($R/L_{nf} \gg 1$) so the thermal ion distribution is hollow ($R/L_{ni} < 0$). And it is important to note that at the ITB location the thermal plasma beta for FIRE is small. All of these features point toward *dilution* as a possible cause of the improved confinement found in FIRE mode. Indeed, in FIRE mode, χ_i decreases considerably - approaching neoclassical levels - and the existence of a transport bifurcation underlying the ITB is evident from an empirically constructed ion heat flux landscape.

All of the above considerations suggest that the effect of EP-induced dilution on drift wave turbulence is a promising route to understanding enhanced confinement in FIRE mode. However, simple linear theory and mixing length type estimates do not offer a satisfactory explanation of the phenomena. Thus, one naturally turns to the question of how EPs impact zonal flows and E×B shearing in plasmas with significant diluteness. This emerges as perhaps the *simplest* means to address the challenge of FIRE mode.

Recently, Hahm *et al.* [17] examined the effects of dilution on zonal flow generation, with an emphasis on dilution effects on interaction resonances. For simplicity and clarity, they focused on the prototypical Hasegawa-Mima model, which is generic. The crux of the issue is that dilution weakens the effect of dispersion on the drift wave frequency, so the well-known dispersion relation $\omega = \omega_*/(1 + k_\perp^2 \rho_s^2)$ becomes $\omega = (1-f)\eta_n \omega_*/[1+(1-f)k_\perp^2\rho_s^2]$, where $\eta_n \equiv L_{ne}/L_{ni}$. As a consequence, the frequency mismatch that must be overcome to allow zonal flow generation is reduced, and zonal flow activity can be expected to be enhanced. There is some subtlety in the matter, as dilution affects couplings, as well, and so enters the generation process in a variety of ways.

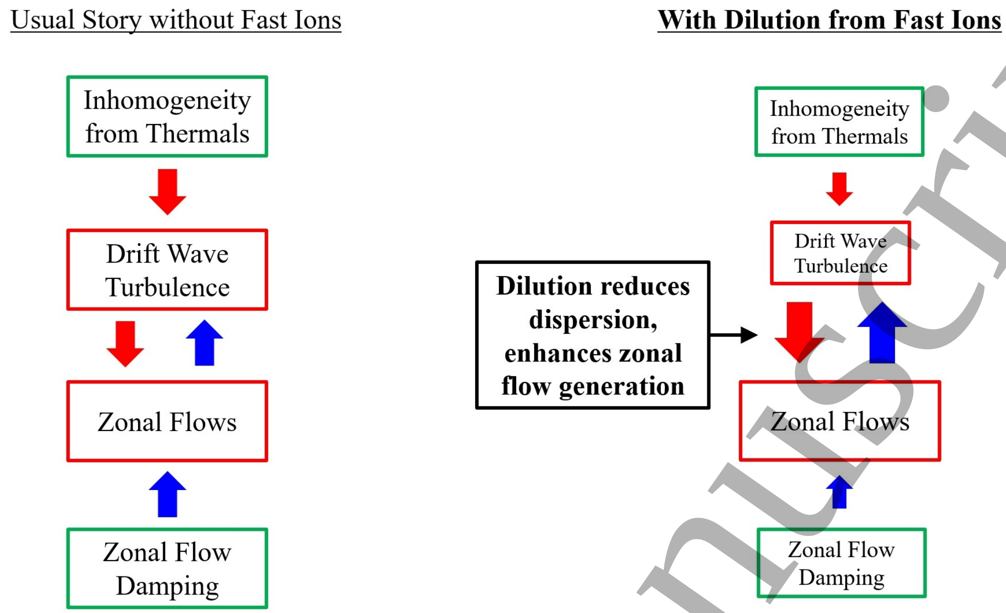

Figure 1. Diagram illustrating the fast ion dilution effect on the drift wave turbulence-zonal flow system. A typical case for core turbulence is illustrated. Note that changes in both box sizes and the thickness of arrows roughly indicate the magnitudes. Red arrows indicate drives and blue arrows indicate suppressing influences. Change in the saturated zonal flow depends on the parameters.

In this paper, we examine the coupled zonal flow and drift wave system in the presence of dilution. Both zonal flow generation and the effect of shearing on a drift wave spectrum are calculated, thus closing the feedback loop. The zonal flow growth rate and the evolution of the drift wave population are calculated self-consistently, using wave kinetics. Both resonant interaction and non-resonant interaction limits are considered. The former is more appropriate for strong turbulence, while the latter is more appropriate for weak turbulence. The weak turbulence limit is clearly more relevant to the core confinement of FIRE mode. The effects of dilution on the frictional damping of zonal flows are also addressed. The upshot is a coupled set of equations for the drift wave and zonal flow energies. Energy conservation is demonstrated in this system. The coupled system can be simplified to the intuitive and familiar form of a predator-prey model. The roots or fixed points of this system describe the basic states of the system. As usual, zonal flow damping is crucial to the regulation of the turbulence intensity for the non-trivial root. Alternatively put, predator damping regulates the prey. A diagram illustrating the fast ion effects on the drift wave-zonal flow system is shown in Fig. 1. A key result of this paper is that the saturated drift wave intensity scales as $\varepsilon_{\mathrm{DW}} \sim \eta_n^2(1-f)^3$ in the weak turbulence regime. Thus, we show dilution and density gradient flattening can strongly reduce drift wave turbulence and the resulting transport, indeed to levels approaching neoclassical. This strengthens the case for dilution as the mechanism underlying the enhanced confinement in FIRE mode, by providing quantitative calculations of turbulence levels.

In this work, we consider the near-zero-frequency zonal flows which are typically the dominant component of the zonal flows in both tokamak and stellarator core plasmas as evidenced from both simulations [18] and experiments [19,20]. The geodesic acoustic mode (GAM) [21] on the other hand, has a well-defined relatively high frequency and therefore is not effective in shearing core turbulence eddies [22]. Its version excited by resonant interaction with the fast ions is called the energetic particle-driven geodesic acoustic mode (EGAM) [23]. It should be however noted that the resonant interaction between the fast ions with a high characteristic frequency and the near-zero-frequency zonal flows is unlikely to occur. So we do not consider the resonant interactions of fast ions and zonal flows

The remainder of this paper is organized as follows. Section 2 presents the theory of zonal flow generation with dilution. The evolution of the drift wave population in the zonal flow shearing field is calculated in Section 3. Energy conservation is shown. The dilution effect on collisional zonal flow damping is discussed in Section 4. Section 5 discusses and solves the predator-prey model, in both the resonant and non-resonant limits. A discussion and Conclusion are given in Section 6. In particular, approaches to validation are suggested and extensions to a model of ITB formation are outlined.

2. Zonal flow generation

Here we consider a simple model system consisting of drift wave and zonal flow with fast ions' contributions based on the Hasegawa-Mima equation, following Ref. [17]. The effect of fast ions is encapsulated in a dilution factor f, which represents the ratio of fast ion charge to electron charge. Fast ions are treated as passive. "Passive" here is effectively equivalent to causing or contributing to dilution. As $k_\parallel v_\parallel \gg \omega$ for energetic particles in drift wave fields, the energetic particles (EPs) to not undergo transport or drive instability. The EPs are dynamically passive, entering via the quasi-neutrality condition only. We start from the modified Hasegawa-Mima equation in the long-wavelength regime $k_\perp^2\rho_s^2 \ll k_\perp^2\rho_{Tf}^2 \ll 1$ and $q^2\rho_s^2 \ll q^2\rho_{Tf}^2 \ll 1$, where $\mathbf{k}$ and $\mathbf{q}$ are wavevectors of the drift wave and zonal flow, and ρ_s and ρ_f are the sound and fast ion gyroradii. In this regime, the modified Hasegawa-Mima equation takes the following form [17].

$$\begin{aligned}&\partial_t\{\tilde{\phi} - (1-f)\nabla^2\tilde{\phi} - \nabla^2\overline{\phi}\} - \boldsymbol{\nabla}\phi\times\hat{z}\cdot\boldsymbol{\nabla}\{\tilde{\phi} - (1-f)\nabla^2\tilde{\phi} - \nabla^2\overline{\phi}\}\\ &+(1-f)\eta_n\partial_y\tilde{\phi} = 0.\end{aligned} \tag{1}$$

This full modified Hasegawa-Mima equation could be decomposed into the zonal flow and the drift wave parts. Then, we have

$$\partial_t\nabla_\perp^2\overline{\phi} - \overline{\boldsymbol{\nabla}\tilde{\phi}\times\hat{z}\cdot\boldsymbol{\nabla}(1-f)\nabla_\perp^2\tilde{\phi}} = 0, \tag{2}$$

for the zonal flow evolution, and

$$\begin{aligned}&\partial_t\{\tilde{\phi} - (1-f)\nabla_\perp^2\tilde{\phi}\} - \boldsymbol{\nabla}\overline{\phi}\times\hat{z}\cdot\boldsymbol{\nabla}\{\tilde{\phi} - (1-f)\nabla_\perp^2\tilde{\phi}\}\\ &+\boldsymbol{\nabla}\tilde{\phi}\times\hat{z}\cdot\boldsymbol{\nabla}\nabla_\perp^2\overline{\phi} + (1-f)\eta_n\partial_y\tilde{\phi} = 0,\end{aligned} \tag{3}$$

for the drift wave evolution, which correspond to Eqs. (11) and (12) of Ref. [17]. Here, we have $\phi = \overline{\phi} + \tilde{\phi}$ where $\overline{\phi}$ and $\tilde{\phi}$ are the zonal flow and the drift wave electric potentials, respectively, where $\overline{(\cdots)}$ denotes the flux-surface average. $\hat{z}$ is the direction of the magnetic field and $\perp$ is for the direction perpendicular to it. $f \equiv Z_f n_{f0}/n_{e0}$ is the fast ion charge density fraction, and $\eta_n \equiv L_{ne}/L_{ni}$ captures relative steepness of the thermal ion density profile compared to the electron one, where $L_{nj} \equiv n_{j0}/|\nabla n_{j0}|$ is the density gradient length of a species j. Note that the potential, space, and time have been normalized by [17]

$$\phi \to \frac{L_{ne}}{\rho_s}\frac{e\phi}{T_e}, \quad \mathbf{x} \to \frac{\mathbf{x}}{\rho_s}, \quad t \to \frac{L_{ne}}{c_s}t. \tag{4}$$

In the present work, we consider the interaction between the zonal flow and broadband drift wave turbulence spectrum rather than coherent interactions between the zonal flow and a few drift waves [17]. Accordingly, for the drift waves, we use the wave-kinetic equation [12,13] which can be constructed from Eq. (3) [12,13,24–28],

$$\partial_t N + \mathbf{v}_g \cdot \boldsymbol{\nabla} N - \boldsymbol{\nabla}(\omega_{\mathbf{k}} + k_y \overline{u}_{\mathrm{E}}) \cdot \frac{\partial N}{\partial \mathbf{k}} = 2\gamma_{\mathbf{k}} N - \frac{\Delta\omega_{\mathbf{k}}}{N_0} N^2, \tag{5}$$

for appropriate treatment of the modulational zonal flow generation [13]. Here, $N(\mathbf{x}, \mathbf{k}, t)$ is the wave action density representing the population of the drift wave quanta, $\mathbf{v}_g = \partial\omega_{\mathbf{k}}/\partial\mathbf{k}$ is the group velocity of the drift waves, $\overline{\mathbf{u}}_{\mathrm{E}} = \overline{u}_{\mathrm{E}}\hat{y}$ is the zonal flow velocity, and $\gamma_{\mathbf{k}}$ and $\Delta\omega_{\mathbf{k}}$ are the linear growth rate and the ambient decorrelation rate of the drift wave turbulence. The drift wave frequency is, with fast ions' contribution [17],

$$\omega_{\mathbf{k}} = \frac{(1-f)\eta_n}{1 + (1-f)k_\perp^2}\omega_*, \tag{6}$$

where $\omega_* = k_y$ is the normalized electron diamagnetic frequency. Note that the effect of dilution is to reduce the effective diamagnetic frequency and to reduce the polarization drift coupling. The latter is especially important since it reduces wave dispersion and thus also lowers the mismatch which must be overcome for resonant interaction of drift waves.

Regarding the zonal flow evolution, we can re-express the second term of Eq. (2) using the Taylor identity [29,30] as follows,

$$\overline{\boldsymbol{\nabla}\tilde{\phi} \times \hat{z} \cdot \boldsymbol{\nabla}(1-f)\nabla_\perp^2\tilde{\phi}} = (1-f)\partial_x^2\overline{(\partial_y\tilde{\phi})(\partial_x\tilde{\phi})}, \tag{7}$$

This relates the flux of the vorticity to the familiar Reynolds stress. Then, using the Fourier representation for drift waves, we can rewrite Eq. (2) as

$$\partial_t\overline{\phi} = (1-f)\sum_{\mathbf{k}} k_x k_y |\tilde{\phi}_{\mathbf{k}}|^2. \tag{8}$$

Considering the initial zonal flow generation, we have $\overline{\phi} = \delta\overline{\phi}$, where δ denotes the modulation. Accordingly, Eq. (8) becomes

$$\partial_t\delta\overline{\phi} = (1-f)\sum_{\mathbf{k}} \frac{k_x k_y \omega_{\mathbf{k}}}{[1 + (1-f)k_\perp^2]}\delta N, \tag{9}$$

where we have used the relation $N = \varepsilon_{\mathbf{k}}/\omega_{\mathbf{k}}$ between the drift wave energy density

$$\varepsilon_{\mathbf{k}} = [1 + (1-f)k_\perp^2]|\tilde{\phi}_{\mathbf{k}}|^2 \tag{10}$$

and the drift wave action density $N(\mathbf{x}, \mathbf{k}, t)$ [24, 28].

Now, we need the response of the wave action density δN. Considering a linearized response for simplicity, from Eq. (5), we have

$$\partial_t \delta N + \mathbf{v}_g \cdot \boldsymbol{\nabla} \delta N - k_y \delta \overline{u}'_{\mathrm{E}} \frac{\partial \langle N \rangle}{\partial k_x} = 2\gamma_{\mathbf{k}} \delta N - 2\frac{\Delta\omega_{\mathbf{k}}}{N_0} \langle N \rangle \delta N. \tag{11}$$

In Eq. (11), we have used $N = \langle N \rangle + \delta N$, where $\langle N \rangle$ and δN are the mean and the modulation parts of the drift wave action density. Here, the mean $\langle N \rangle$ is a coarse-grained part of N spatially averaging the mesoscale modulation as an approximation of an ensemble average. Fourier-decomposing $\delta N = \sum_{q,\Omega} \delta N_q \exp[i(qx - \Omega t)]$ and similarly for $\delta \overline{u}_{\mathrm{E}}$, we obtain

$$\delta N_q = iqk_y \delta \overline{u}_{\mathrm{E}q} R_q \frac{\partial \langle N \rangle}{\partial k_x} = -q^2 k_y R_q \frac{\partial \langle N \rangle}{\partial k_x} \delta \overline{\phi}_q, \tag{12}$$

where

$$R_q \equiv (-i\Omega + iqv_{gx} + \Lambda)^{-1} \tag{13}$$

is the propagator where $\Lambda \equiv -2\gamma_{\mathbf{k}} + 2\Delta\omega_{\mathbf{k}} \langle N \rangle / N_0$. Hereafter, we consider spatially homogeneous mean drift wave action density $\langle N \rangle(\mathbf{k}, t)$. Then, with $\langle N \rangle \simeq N_0$, we have $2\gamma_{\mathbf{k}} = \Delta\omega_{\mathbf{k}}$ and $\Lambda \simeq 2\gamma_{\mathbf{k}} \simeq \Delta\omega_{\mathbf{k}}$. Details will be shown in the next section.

Substituting Eq. (12) into Eq. (9), we obtain

$$\partial_t \delta \overline{\phi}_q = -(1-f)^2 \eta_n q^2 \sum_{\mathbf{k}} \frac{k_y^2 \omega_*}{[1 + (1-f)k_\perp^2]^2} R_q k_x \frac{\partial \langle N \rangle}{\partial k_x} \delta \overline{\phi}_q. \tag{14}$$

Note that one $(1-f)$ factor in Eq. (14) originating from the drift wave frequency $\omega_{\mathbf{k}}$ in Eq. (9) will cancel with the $1/(1-f)$ dependence of the drift wave action density N as will be shown in the next section.

First, we consider the limit $|\Omega - qv_{gx}| \ll \gamma_{\mathbf{k}}$ which we call the resonant interaction regime in this paper. Here, resonance refers to that between the zonal modulator frequency Ω and the drift wave ballistic frequency qv_{gx}. The resonant regime may be thought of as a "strong turbulence" regime. A detailed explanation is presented in Appendix A. The zonal flow growth rate is given by

$$\Gamma = -(1-f)q^2 \sum_{\mathbf{k}} \frac{k_y^2 (1-f) \eta_n \omega_*}{[1 + (1-f)k_\perp^2]^2} \frac{1}{2|\gamma_{\mathbf{k}}|} k_x \frac{\partial \langle N \rangle}{\partial k_x}. \tag{15}$$

In Eq. (15), we have a common $(1-f)$ dependence of the zonal flow growth rate Γ originating from a reduction of the Reynolds stress in Eq. (8).

The factor $1/|\gamma_{\mathbf{k}}|$ in Eq. (15) however can exhibit various behaviors, as the dependence of the turbulence linear growth rate on fast ions is specific to macroscopic parameters, as reported from gyrokinetic simulation studies [31–35]. A stabilizing role of inverted density profile on the ion temperature gradient (ITG) mode is well-known from simple linear analyses [36, 37]. It has been found that the fast ion dilution stabilizes the trapped electron mode (TEM) for high L_{ne}/L_{Te} [31] but destabilizes for low L_{ne}/L_{Te} [32]. Also, the wave-particle resonance with fast ions stabilizes the ITG mode with low L_{nf}/L_{Tf} [33] but destabilizes with high L_{nf}/L_{Tf} [34]. Recently, ITG mode stabilization by fast ion dilution has been studied in detail [35].

The $1/|\gamma_{\mathbf{k}}|$ dependence of Eq. (15) indicates that the zonal flow generation could be more efficient with fast ions if there is strong fast ion-induced linear stabilization of drift wave turbulence. This is because $1/|\gamma_{\mathbf{k}}|$ ultimately controls the correlation time of the zonal modulation with the drift wave action response. As a result, there could be a significant nonlinear zonal flow generation even with considerably weakened turbulence by fast ions. This will further lower the turbulence level.

On the other hand, in the non-resonant, or weak turbulence regime, with $|\Omega - qv_{gx}| \gg \gamma_{\mathbf{k}}$, Eq. (14) can be approximated as

$$\Omega = (1-f)q^2 \sum_{\mathbf{k}} \frac{k_y^2(1-f)\eta_n\omega_*}{[1+(1-f)k_\perp^2]^2} \frac{1}{\Omega - qv_{gx}} k_x \frac{\partial \langle N \rangle}{\partial k_x}, \tag{16}$$

where the expression of the radial group velocity of the drift wave is

$$v_{gx} = \frac{\partial \omega_{\mathbf{k}}}{\partial k_x} = -\frac{2(1-f)^2\eta_n\omega_* q k_x}{[1+(1-f)k_\perp^2]^2}. \tag{17}$$

It is important to note that the radial group velocity v_{gx} gives a finite threshold for the zonal flow generation. Heuristically, Eq. (16) could be rearranged as follows [13], neglecting the wavevector dependence of v_{gx}.

$$\Omega(\Omega - qv_{gx}) \approx -\gamma_{\mathrm{mod}}^2, \tag{18}$$

where

$$\gamma_{\mathrm{mod}}^2 \approx -(1-f)q^2 \sum_{\mathbf{k}} \frac{k_y^2(1-f)\eta_n\omega_*}{[1+(1-f)k_\perp^2]^2} k_x \frac{\partial \langle N \rangle}{\partial k_x}, \tag{19}$$

characterizes the modulational zonal flow drive. Then, the zonal flow dispersion relation, Eq. (18), yields

$$\Gamma \approx \sqrt{\gamma_{\mathrm{mod}}^2 - (qv_{gx})^2}. \tag{20}$$

Note that on the RHS of Eq. (20), the modulational drive γ_{mod}^2 is reduced by $(1-f)$ due to the dilution-induced reduction of the Reynolds stress. However, the finite threshold given by the drift wave dispersion $(qv_{gx})^2$ decreases much more significantly with $(1-f)^4$. This is due to the effects of dilution on the drift wave frequency and thus on the group velocity. As a consequence, the critical turbulence amplitude for the zonal flow generation is significantly lowered by fast ions. Far from marginality, we have $\Gamma \propto \sqrt{1-f}$ indicating that the fast ion dilution reduces the zonal flow growth. The fast ion dilution effects on the zonal flow generation in this limit are quantitatively consistent with previous theoretical work presented in Ref. [17] based on the 4-wave-coupling analysis, except for the zonal flow wavenumber q-dependence of the threshold.

3. Drift wave evolution in the presence of zonal flows

In this section, drift wave evolution in the presence of zonal flows is presented. Taking the mean part of Eq. (5), with $\langle N\rangle(\mathbf{k},t)$, we have

$$\partial_t\langle N\rangle - \left\langle k_y(\partial_x\overline{u}_{\mathrm{E}})\frac{\partial\delta N}{\partial k_x}\right\rangle = 2\gamma_{\mathbf{k}}\langle N\rangle - \frac{\Delta\omega_{\mathbf{k}}}{N_0}\langle N\rangle^2 - \frac{\Delta\omega_{\mathbf{k}}}{N_0}\langle(\delta N)^2\rangle. \tag{21}$$

We divide $\langle N\rangle = N_0(\mathbf{k}) + N_1(\mathbf{k},t)$, where $N_0(\mathbf{k})$ is the homogeneous stationary solution of the wave kinetic equation describing the ambient drift wave turbulence in the absence of the zonal flow. Then, we rewrite Eq. (21) as

$$\begin{aligned}\partial_t N_1 - \left\langle k_y(\partial_x\overline{u}_{\mathrm{E}})\frac{\partial\delta N}{\partial k_x}\right\rangle &= 2\gamma_{\mathbf{k}}N_0 - \Delta\omega_{\mathbf{k}}N_0\\ &+ 2\gamma_{\mathbf{k}}N_1 - 2\Delta\omega_{\mathbf{k}}N_1 - \frac{\Delta\omega_{\mathbf{k}}}{N_0}N_1^2 - \frac{\Delta\omega_{\mathbf{k}}}{N_0}\langle(\delta N)^2\rangle.\end{aligned} \tag{22}$$

In the limit of no zonal flow, we obtain $2\gamma_{\mathbf{k}} = \Delta\omega_{\mathbf{k}}$. Substituting it into Eq. (22), we have

$$\partial_t N_1 - \left\langle k_y(\partial_x\overline{u}_{\mathrm{E}})\frac{\partial\delta N}{\partial k_x}\right\rangle = -\Delta\omega_{\mathbf{k}}N_1 - \frac{\Delta\omega_{\mathbf{k}}}{N_0}N_1^2 - \frac{\Delta\omega_{\mathbf{k}}}{N_0}\langle(\delta N)^2\rangle. \tag{23}$$

Here, we have two terms originating from the modulation; the second term on the left-hand side (LHS) and the last term on the RHS. With an auxiliary ordering

$$\frac{N_1}{N_0} \ll \frac{k_y^2 q^2 u_{\mathrm{E}}^2|R_q|}{\Delta\omega_{\mathbf{k}}\Delta k_x^2}, \tag{24}$$

where Δk_x is the width of the broadband drift wave spectrum, we neglect the first term and accordingly the second term on the RHS of Eq. (23) as we are interested in the initial zonal flow growth. We also neglect the third term based on $\Delta\omega_{\mathbf{k}}|R_q| < 1$. Then, we obtain

$$\partial_t\langle N\rangle \simeq \frac{\partial}{\partial k_x}\langle k_y(\partial_x\delta\overline{u}_{\mathrm{E}})\delta N\rangle = \frac{\partial}{\partial k_x}\left[\sum_q q^2k_y^2|\delta\overline{u}_{\mathrm{E}q}|^2\mathrm{Re}(R_q)\right]\frac{\partial\langle N\rangle}{\partial k_x}. \tag{25}$$

The bracket $[\cdots]$ on the RHS of Eq. (25) represents the spectral diffusion in k_x space by zonal flow-induced random shearing. Here, the shearing rate and the propagator correspond to the step size for Δk_x and the shearing field-wave packet correlation time, respectively. Eq. (25) is yet another appearance of the familiar induced diffusion equation for $\langle N\rangle$ in k_x space. Eq. (25) validity requires overlap of $\Omega = qv_{gx}$ resonances. The origin of the irreversibility that underlies induced diffusion is the chaos of drift wave rays.

Now, we consider the evolution of the mean drift wave energy $\langle\varepsilon\rangle = \sum_{\mathbf{k}}\langle\varepsilon_{\mathbf{k}}\rangle$ to show that our wave-kinetic approach is consistent with the energy conservation. Multiplying Eq. (25) by $\omega_{\mathbf{k}}$ and taking $\mathbf{k}$-space integration, we have

$$\partial_t\langle\varepsilon\rangle = \int d^3\mathbf{k}\,\omega_{\mathbf{k}}\frac{\partial}{\partial k_x}\left[\sum_q q^2k_y^2|\delta\overline{u}_{\mathrm{E}q}|^2\mathrm{Re}(R_q)\right]\frac{\partial\langle N\rangle}{\partial k_x} \tag{26}$$

$$= -\int d^3\mathbf{k}\, v_{gx} \left[\sum_q q^2 k_y^2 |\delta\overline{u}_{\mathrm{E}q}|^2 \mathrm{Re}(R_q) \right] \frac{\partial \langle N \rangle}{\partial k_x} \tag{27}$$

$$= \sum_q \int d^3\mathbf{k} \frac{2(1-f)^2 \eta_n \omega_*}{[1+(1-f)k_\perp^2]^2} q^2 k_y^2 |\delta\overline{u}_{\mathrm{E}q}|^2 \mathrm{Re}(R_q) k_x \frac{\partial \langle N \rangle}{\partial k_x}. \tag{28}$$

By multiplying Eq. (14) by $\delta\overline{u}_{\mathrm{E}-q}$ and taking the q-space sum, we obtain

$$\partial_t \langle \overline{u}_{\mathrm{E}}^2 \rangle = -\sum_q \int d^3\mathbf{k} \frac{2(1-f)^2 \eta_n \omega_*}{[1+(1-f)k_\perp^2]^2} q^2 k_y^2 |\delta\overline{u}_{\mathrm{E}q}|^2 \mathrm{Re}(R_q) k_x \frac{\partial \langle N \rangle}{\partial k_x}. \tag{29}$$

From Eqs. (28) and (29), we obtain the energy conservation relation for the drift wave-zonal flow interaction,

$$\partial_t \left[\langle \varepsilon \rangle + \langle \overline{u}_{\mathrm{E}}^2 \rangle \right] = 0. \tag{30}$$

The energy conservation could also be derived directly from the full modified Hasegawa-Mima equation, Eq. (1). Multiplying ϕ to Eq. (1) and integrating over the system, we readily obtain the global energy conservation law [17]

$$\frac{d}{dt} \int d^3\mathbf{x} \frac{1}{2} \left[\tilde{\phi}^2 + (1-f)|\nabla\tilde{\phi}|^2 + |\nabla\overline{\phi}|^2 \right] = 0, \tag{31}$$

which is consistent with Eq. (30). Note that Eqs. (30) and (31) confirm that Eq. (10) is a proper expression of the drift wave energy density $\varepsilon_{\mathbf{k}}$, which does not have an overall proportionality to the dilution factor $(1-f)$. Accordingly, the drift wave action density N significantly changes with fast ion population by $N = \varepsilon_{\mathbf{k}}/\omega_{\mathbf{k}} \propto 1/(1-f)$.

4. Changes in collisional damping of zonal flows due to fast ions

While our main interest in this paper is the nonlinear interaction of zonal flows and drift wave turbulence in the presence of fast ions, both changes in collisional linear damping of zonal flows and linear growth rate of drift instabilities due to fast ions can contribute to the nonlinearly saturated turbulence level and anomalous transport carried by it. We present a simple characterization of the former in this section so that it can be incorporated into the extended Predator-Prey model including the fast ions' effect presented in Sec. 5.

Regarding collisional damping of zonal flows, it should be remembered that the mass flow in a symmetric direction can be sustained for a long time in the absence of turbulent damping because it can only be damped by the collisional viscosity [38]. So the zonal flows in a cylindrical geometry which is in the poloidal direction will be damped with a rate proportional to

$$\mu_{\mathrm{visc}(0)} \simeq \nu_{ii} \rho_i^2 q_r^2. \tag{32}$$

Then by characterizing the fast ions with their own temperature T_f, we expect their contribution will reduced the viscous damping by

$$\mu_{\mathrm{visc}} \simeq (1-f) \mu_{\mathrm{visc}(0)}, \tag{33}$$

for $T_f/T_i \gg 1$, noting $\nu_{ii} \propto T_i^{-3/2}$.

In toroidal plasmas, the collisional viscosity is neoclassically enhanced by a factor $\sim q^2$ (here q is the safety factor, not zonal flow wavenumber, as in the rest of this paper) without an inverse aspect ratio dependence even in the banana collisionality regime [38], but the fast ion effect is still characterized by Eq. (33). More importantly, the zonal flows' collisional damping mainly in the poloidal direction can come from the friction between trapped ions and passing ions in the form of a drag [38]. According to Ref. [39], most of the damping occurs during a period $\tau_{\rm HR} \simeq 1.5\epsilon/\nu_{ii}$, where $\epsilon = r/R_0$ is the local inverse aspect ratio. Once again a simple characterization of fast ion population by T_f and a scaling argument lead to an estimation that

$$\gamma_d \simeq (1-f)\nu_{ii(0)}/1.5\epsilon = (1-f)\gamma_{d(0)}, \tag{34}$$

where $\gamma_{d(0)} \equiv \nu_{ii(0)}/1.5\epsilon$, and $T_f/T_i \gg 1$ has been assumed.

So with these caveats in mind, we use Eq. (34) for our characterization of the fast ions' effect on collisional damping of zonal flows.

5. Extended predator-prey model for drift wave-zonal flow system

In previous sections, various aspects of the drift wave-zonal flow interaction have been studied in the presence of fast ions. These include the zonal flow generation by drift wave turbulence in Sec. 2, the back reaction of zonal flows on drift waves in Sec. 3, and the collisional (linear) damping of zonal flows in Sec. 4. In this section, we study the self-consistent states of the system with the aforementioned processes as building blocks. *This will lead us to an overall assessment of the fast ion effects on turbulence, while most previous studies considered only a part of the whole story in detail.*

5.1. Resonant interaction (strong turbulence) regime

The simplest model describing this interacting system is the predator-prey model. First, we consider a strong turbulence regime $|\Omega - qv_{gx}| \ll \gamma_{\mathbf{k}}$. The excitation of zonal flow by drift waves is described by Eq. (15), while the collisional damping is given by Eq. (34). Combining these, we have a zonal flow evolution equation,

$$\partial_t |u_{\rm ZF}|^2 = (1-f)A\varepsilon_{\rm DW}|u_{\rm ZF}|^2 - (1-f)\gamma_{d(0)}|u_{\rm ZF}|^2. \tag{35}$$

Here, using $N = \varepsilon_{\mathbf{k}}/\omega_{\mathbf{k}}$,

$$A \equiv -q^2 \sum_{\mathbf{k}} \frac{k_y^2\eta_n}{[1+(1-f)k_\perp^2]^2}\left[\frac{(1-f)\omega_*}{\omega_{\mathbf{k}}}\right]\frac{1}{2|\gamma_{\mathbf{k}}|}\frac{k_x}{\langle N\rangle}\frac{\partial\langle N\rangle}{\partial k_x}. \tag{36}$$

The form of Eq. (35) is similar to that derived previously in Ref. [13] but with dilution effects included. Note that, with Eq. (6), we expect $[(1-f)\omega_*/\omega_{\mathbf{k}}]$ in Eq. (36) to be independent of $(1-f)$ in the long-wavelength limit. Therefore, the fast ion effect on the drift wave-zonal flow coupling coefficient A mostly comes from $1/|\gamma_{\mathbf{k}}|$ which is strongly case-dependent as discussed in Sec. 2.

The drift wave evolution under the random shearing by zonal flows is given by Eq. (28). We note that an identical expression of the coefficients in Eq. (15) and Eq. (28) is closely related to the energy conservation between drift waves and zonal flows in the absence of growth and damping. Adding the linear growth rate and the expected nonlinear mode couplings among drift waves, we can write the drift wave evolution equation as,

$$\partial_t \varepsilon_{\mathrm{DW}} = 2\gamma\varepsilon_{\mathrm{DW}} - (1-f)A|u_{\mathrm{ZF}}|^2\varepsilon_{\mathrm{DW}} - (1-f)B\varepsilon_{\mathrm{DW}}^2. \tag{37}$$

An explicit formula for B is available from the literature, for instance, [40]. Eq. (37) also closely resembles previous corresponding equations but with dilution effects included. Note that $(1-f)$ in the turbulence decorrelation rate $(1-f)B\varepsilon_{\mathrm{DW}}$ originates from the reduced drift wave vorticity in the Hasegawa-Mima nonlinearity [17]. With non-adiabatic electrons, the E×B nonlinearity enters [41] making the dilution effect on the turbulence decorrelation complex, but this detail is outside of the scope of this paper.

It is well-known that a system of Eqs. (35) and (37) yields two types of steady-state solution. In the case of strong zonal flow damping, i.e.,

$$(1-f)\gamma_{d(0)} > \frac{2\gamma A}{B}, \tag{38}$$

we get the solution for the case without zonal flow,

$$|u_{\mathrm{ZF}}|^2 = 0, \quad \text{and} \quad \varepsilon_{\mathrm{DW}} = \frac{2\gamma}{(1-f)B}. \tag{39}$$

For weaker zonal flow damping

$$(1-f)\gamma_{d(0)} < \frac{2\gamma A}{B}, \tag{40}$$

zonal flows and drift waves coexist with values at nonlinear saturation given by

$$\varepsilon_{\mathrm{DW}} = \frac{\gamma_{d(0)}}{A}, \tag{41}$$

and

$$|u_{\mathrm{ZF}}|^2 = \frac{1}{A}\left[2\gamma - \frac{(1-f)B\gamma_{d(0)}}{A}\right]. \tag{42}$$

Eqs. (41) and (42) exhibit large cancellations of the $(1-f)$ factors coming from different terms resulting in a weak dependence of nonlinear saturation levels of drift waves and zonal flows on dilution. Note that Eq. (41) has the familiar 'predator-prey structure' of fluctuation level proportional to zonal flow damping. Case-specific reduction of drift wave turbulence by fast ions is feasible through the manipulation of the linear growth rate γ and thus zonal flow coupling coefficient $A[\gamma]$, but no universal trend is anticipated in the strong turbulence regime.

One might conclude that this result is in contrast to the highly publicized recent experimental findings of confinement improvements caused by fast ions [8, 16]. But we should notice that the strong turbulence ordering $|\Omega - qv_{gx}| \ll \gamma$ is more likely to be justified for the edge turbulence rather than the core turbulence (in the presence of an internal transport barrier (ITB)). Indeed, most core enhanced confinement modes are not accompanied by simultaneous confinement improvement at the edge leading to H-mode transition. Specific examples include KSTAR [16], JET [8], TFTR [42, 43], and JT60-U [44, 45].

5.2. Non-resonant interaction (weak turbulence) regime

In the weak turbulence regime with $|\Omega - qv_{gx}| \gg \gamma_{\mathbf{k}}$, Eq. (16) suggests an evolution equation of the zonal flow in a form

$$\partial_t(\partial_t - iqv_{gx})|u_{\mathrm{ZF}}|^2 = \cdots \tag{43}$$

which is difficult for further analytic progress. Instead, we seek a simpler model based on Eq. (20), i.e.,

$$\partial_t|u_{\mathrm{ZF}}|^2 = \sqrt{\gamma_{\mathrm{mod}}^2 - \Delta_{\mathrm{mm}}^2}H(\gamma_{\mathrm{mode}} - \Delta_{\mathrm{mm}})|u_{\mathrm{ZF}}|^2 - (1-f)\gamma_{d(0)}|u_{\mathrm{ZF}}|^2, \tag{44}$$

where $\gamma_{\mathrm{mod}}^2 \to (1-f)A'\varepsilon_{\mathrm{DW}}$ from Eq. (19),

$$A' \equiv -q^2 \sum_{\mathbf{k}} \frac{k_y^2 \eta_n}{[1 + (1-f)k_\perp^2]^2} \left[\frac{(1-f)\omega_*}{\omega_{\mathbf{k}}}\right] \frac{k_x}{\langle N \rangle} \frac{\partial \langle N \rangle}{\partial k_x}, \tag{45}$$

and H is the Heaviside function. Here, the continuum limit expression in the wave-kinetic approach, $(qv_{\mathrm{gx}})^2$, has been replaced by the original frequency mismatch $\Delta_{\mathrm{mm}}^2 = (1-f)^4\Delta_{\mathrm{mm}(0)}^2$ where $\Delta_{\mathrm{mm}(0)}^2 = q^4 \sum_{\mathbf{k}} \eta_n^2 k_y^2$ [17]. Note that it can only reduce the zonal flow growth rate down to zero, and cannot make the zonal flow growth negative by itself.

The corresponding drift wave energy evolution equation in this regime, which satisfies the energy conservation relation in Eq. (30), is then

$$\partial_t\varepsilon_{\mathrm{DW}} = 2\gamma\varepsilon_{\mathrm{DW}} - \sqrt{\gamma_{\mathrm{mod}}^2 - \Delta_{\mathrm{mm}}^2}H(\gamma_{\mathrm{mode}} - \Delta_{\mathrm{mm}})|u_{\mathrm{ZF}}|^2 - (1-f)B\varepsilon_{\mathrm{DW}}^2. \tag{46}$$

According to Eqs. (44) and (46), there is a trivial solution with no zonal flow,

$$|u_{\mathrm{ZF}}|^2 = 0, \quad \text{and} \quad \varepsilon_{\mathrm{DW}} = \frac{2\gamma}{(1-f)B}, \tag{47}$$

for the case of a strong zonal flow damping $\gamma_d^2 > \gamma_{\mathrm{mod}}^2 - \Delta_{\mathrm{mm}}^2$, that is,

$$(1-f)^2\gamma_{d(0)}^2 > \frac{2\gamma A'}{B} - (1-f)^4\eta_n^2\Delta_{\mathrm{mm}(0)}^2. \tag{48}$$

In addition, there exists a non-trivial steady-state solution in which the zonal flow and drift wave turbulence co-exist. In this case, the nonlinear saturation level of the drift wave determined by Eq. (44) should satisfy

$$\gamma_{\mathrm{mod}}^2 = \Delta_{\mathrm{mm}}^2 + \gamma_d^2. \tag{49}$$

This leads to

$$\varepsilon_{\mathrm{DW}} = \frac{(1-f)\gamma_{d(0)}^2}{A'}\left(1 + \frac{(1-f)^2\eta_n^2\Delta_{\mathrm{mm}(0)}^2}{\gamma_{d(0)}^2}\right), \tag{50}$$

and

$$|u_{\mathrm{ZF}}|^2 = \frac{\gamma_{d(0)}}{A'}\left[2\gamma - \frac{(1-f)^2 B\gamma_{d(0)}^2}{A'}\left(1 + \frac{(1-f)^2\eta_n^2\Delta_{\mathrm{mm}(0)}^2}{\gamma_{d(0)}^2}\right)\right] \times\left(1 + \frac{(1-f)^2\eta_n^2\Delta_{\mathrm{mm}(0)}^2}{\gamma_{d(0)}^2}\right), \tag{51}$$

for the case of a weak zonal flow damping

$$(1-f)^2\gamma_{d(0)}^2 < \frac{2\gamma A'}{B} - (1-f)^4\eta_n^2\Delta_{\mathrm{mm}(0)}^2. \tag{52}$$

Note that we expect a favorable role of the energetic particle-induced dilution for confinement quantified by the $(1-f)$ factor from Eq. (50), especially in the collisionless limit in which $\Delta_{\mathrm{mm}(0)}^2 \gg \gamma_{d(0)}^2$ which is applicable to core plasmas, i.e.,

$$\varepsilon_{\mathrm{DW}} \approx \frac{(1-f)^3\eta_n^2\Delta_{\mathrm{mm}(0)}^2}{A'}, \tag{53}$$

and

$$|u_{\mathrm{ZF}}|^2 \approx \frac{(1-f)^2\eta_n^2\Delta_{\mathrm{mm}(0)}^2}{A'\gamma_{d(0)}}\left[2\gamma - \frac{(1-f)^4 B\eta_n^2\Delta_{\mathrm{mm}(0)}^2}{A'}\right]. \tag{54}$$

This trend is consistent with the well-known core confinement enhancement observed in the energetic particle-dominated tokamak plasmas [8, 16, 42]. Note that unlike the case-specific fast ion effect shown in Eq. (41) in the resonant regime, here in Eq. (53) we have a significant universal reduction of saturated turbulence level due to fast ion dilution by a factor of $(1-f)^3$. In addition, the relieved thermal ion density profile gradient due to dilution further reduces the turbulence level by the factor $\eta_n^2 < 1$. Eqs. (53) and (54) are among the principal results of this paper.

Fig. 2 shows the linear growth rate γ dependence of the saturated drift wave and zonal flow energies, for different f and η_n, of which expressions have been shown in Eqs. (41), (42), (53) and (54). For the plot, we have used $A \approx A'/2\gamma$ from Eqs. (36) and (45). In Fig. 2(a), we find that in the strong turbulence (resonant interaction) regime, the fast ion dilution could reduce the saturated drift wave level only through the linear stabilization of drift wave turbulence. Meanwhile in the weak turbulence (non-resonant interaction) regime, more relevant to the core plasma with enhanced confinement, the linear stabilizers have little influence in reducing the saturated turbulence energy. We instead find a universal reduction of the saturated turbulence level by the direct impact of the fast ion fraction $f > 0$ and the reduced thermal ion density gradient $\eta_n < 1$. It is worth noting that for all cases with linear turbulence stabilization, the fast ion dilution decreases the total saturated energy by reducing both turbulence and zonal flow. Fig. 3, showing the saturated drift wave and zonal flow energies depending on f, confirms the reciprocal influence of γ and f (and η_n) on the turbulence suppression in the two different turbulence regimes.

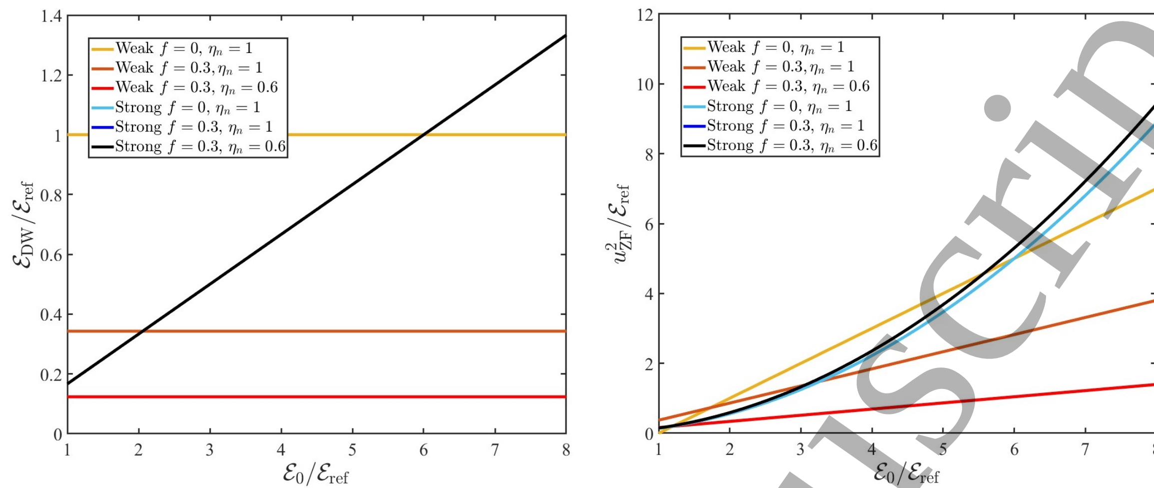

Figure 2. Dependence of the saturated (a) drift wave and (b) zonal flow energies on the linear growth rate $\gamma \propto \mathcal{E}_0$ in weak (non-resonant) and strong (resonant) turbulence regimes, for different fast ion fraction f and relative thermal ion density gradient η_n. Here, $\mathcal{E}_0 = 2\gamma/B$ is the saturated drift wave energy without zonal flow in the absence of fast ions, and $\mathcal{E}_{\mathrm{ref}} = \Delta^2_{\mathrm{mm}0}/A'$ is a collisionless limit form of the saturated drift wave energy with zonal flow in weak turbulence regime in the absence of fast ions.

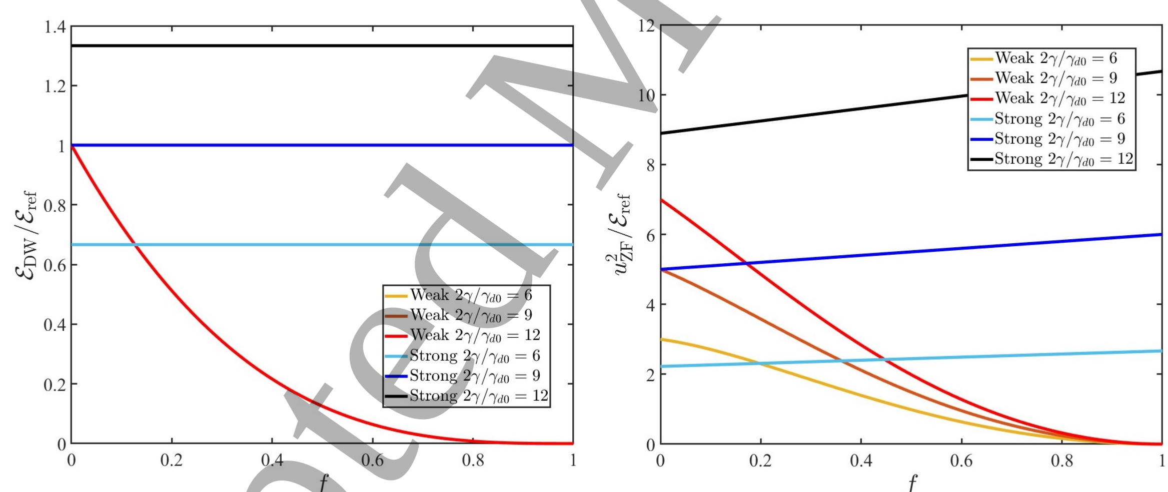

Figure 3. Dependence of the saturated (a) drift wave and (b) zonal flow energies on the fast ion density fraction f in weak and strong turbulence regimes, for different linear growth rate γ. Here, η_n is set to unity for simple illustrations.

A connection to transport remains to be established. Eqs. (53) and (54) determine the level of saturated drift wave fluctuations and zonal flows. The effective diffusion coefficient for drift wave turbulence is given by:

$$D = \sum_{\mathbf{k}} |\tilde{v}_{r\mathbf{k}}|^2 R_{\mathbf{k}}, \tag{55a}$$

where the response operator $R_{\mathbf{k}}$ is given by:

$$R_{\mathbf{k}} = \frac{\Delta\omega_{\mathbf{k}}}{(\omega_{\mathbf{k}} - k_y u_{\mathrm{ZF}})^2 + \Delta\omega^2_{\mathbf{k}}}. \tag{55b}$$

Here, $\Delta\omega_{\mathbf{k}} = 1/\tau_{c\mathbf{k}}$ is the linewidth associated with the correlation time $\tau_{c\mathbf{k}}$ of mode $\mathbf{k}$. Eq. (55a) incorporates the effects of Doppler shift and possible wave-zonal flow resonance absorption. In the strong turbulence limit

$$D \simeq \sum_{\mathbf{k}} \frac{|\tilde{v}_{r\mathbf{k}}|^2}{\Delta\omega_{\mathbf{k}}}. \tag{55c}$$

In the resonant, weak turbulence limit ($\Delta\omega_{\mathbf{k}} < \Delta\omega$)

$$D \simeq \sum_{\mathbf{k}} |\tilde{v}_{r\mathbf{k}}|^2 \pi\delta(\omega - k_y u_{\mathrm{ZF}}) \simeq \sum_{\mathbf{k}} |\tilde{v}_{r\mathbf{k}}|^2 \tau_{\mathrm{ac}}, \tag{55d}$$

where τ_{ac} is the wave-particle auto-correlation time, determined by the spectral width $\Delta\omega$, which is distinct from the linewidth $\Delta\omega_{\mathbf{k}}$. More explanation of the two limits is presented in Appendix B. The resonant, weak turbulence limit is the relevant one for regimes of significant dilution and enhanced confinement.

Thus, we see that transport tracks fluctuation energy density $\sim \langle \tilde{v}^2 \rangle \sim \varepsilon_{\mathrm{DW}}$ and so also scales with $(1-f)^3$. We note that not only the main ion fraction dilution $(1-f)$ but also the reduction of the main ion density gradient quantified by $\eta_n = L_{ne}/L_{ni}$ contribute to the turbulence level and transport. This observation indicates the favorable role of a centrally peaked fast ion profile and suggests that the predator-prey model developed here should be extended to 1D, including profile evolution. This is discussed further in the conclusion.

Finally, we note that the effects discussed here can be quantitatively significant. For the recently discovered KSTAR FIRE mode [16], estimates suggest $f \sim 0.3$, so $(1-f)^3 \sim 0.3$ making for a drastic reduction in D, to levels which may not be so easily distinguished from neoclassical.

6. Conclusion

Interest in the effects of an energetic particle component on plasma confinement and transport grows steadily. In this paper, we analyze perhaps the simplest incarnation of a model of this system - namely drift wave turbulence, with dilution effects due to energetic particles. Here, dilution, represented by the presence of finite $f = Z_f n_{f0}/n_{e0}$, modifies couplings and dispersion in the governing drift wave equations. Otherwise, the fast particles are treated as passive, but do enter charge balance. The principal results of this paper are:

i) the expressions for the modulational growth of zonal flows in a broadband gas of drift waves modified by dilution. These are Eq. (15) and Eqs. (19)-(20), for resonant and non-resonant limits, respectively. Loosely speaking, the resonant limit corresponds to strong turbulence while the non-resonant limit to weak turbulence. The latter is more relevant to enhanced confinement regimes.

ii) the induced diffusion (quasilinear) equation for the drift wave action density in the presence of a zonal flow spectrum, as in Eq. (25). Energy conservation is demonstrated for the system of drift waves and zonal modes.

iii) zonal flow damping due to collisional friction is shown to be modified by dilution. This is important since zonal flow damping regulates the system.

iv) the coupled zonal flow growth and induced diffusion equations are combined and used to derive a predator-prey type model for the evolution of the drift wave-zonal flow system. This is specialized to both the resonant interaction (strong turbulence) and non-resonant (weak turbulence) cases. The fixed point solutions are given by Eqs. (39), (41), (42) and Eqs. (47), (50), (51) respectively.

v) in particular, the drift wave energy saturation level in the weak turbulence regime is derived on Eq. (53), and is $\varepsilon_{\rm DW} = (1-f)^3 \eta_n^2 \Delta^2_{\rm mm(0)}/A'$. The weak turbulence regime is likely most relevant to core turbulence, especially in cases of stronger dilution. Results show a strong effect of dilution $\sim (1-f)^3$, leading to greatly reduced saturated turbulence levels. These in turn reduce the level of transport, and so improve confinement. Dilution is thus seen as a likely cause of confinement improvement in recent experiments with a large fraction of energetic particles.

It is noteworthy that several nonlinear gyrokinetic simulations reported considerable levels of zonal flow shear and significantly reduced drift wave turbulence levels and transport in the presence of fast ions. These trends are in agreement with our theoretical predictions in this paper. These include simulations using parameters based on the experiments on ASDEX-U [34], JET [8] and KSTAR [35].

This paper offers several testable predictions, including both the relation of transport and turbulence intensity to dilution, and the associated change in zonal flow energy and mean square shear. The latter suggests a highly relevant validation test, namely to compare the core zonal flow intensity and structure in FIRE mode, with the corresponding L-mode pattern. This is easily accomplished by Electron Cyclotron Emission Imaging (ECEI) [46] and Beam Emission Spectroscopy (BES) [47]. Furthermore, BES velocimetry could be implemented to determine the flux $\langle \tilde{v}_r \tilde{n} \rangle$ and the turbulence spreading flux $\langle \tilde{v}_r \tilde{n}\tilde{n} \rangle$. The latter has recently been measured by BES velocimetry on the DIII-D tokamak [48]. Here it should be noted that $\tilde{v}_r$ is more akin to a particle velocity than an E×B velocity. Nevertheless, $\langle \tilde{v}_r \tilde{n} \rangle$ is indicative of transport, and $\langle \tilde{v}_r \tilde{n}\tilde{n} \rangle$ is indicative of spreading, avalanching etc and thus of mesoscopic relaxation activity [49]. Both should drop as zonal and mean E×B shear increases. Such a study would constitute a more discriminating validation test than the usual simplistic χ_i comparisons.

It is also worthwhile to note that dilution effects can be expected to modify the structure of mesoscopic structures, such as E×B staircases [50]. Note that since dilution weakens dispersion, it necessarily will modify the effective Rhines scale [51] for the system. This will in turn reduce the emergent mixing scale. Recall that staircases can be formed by a bistable mixing process [52, 53], and that the emergent mixing scale will set the effective step size. Thus dilution-induced modification of staircase structure is to be expected.

At this point, we arrive at the inevitable question of "what next"? The analysis so far ignores the evolution of thermal plasma profiles and of *mean* electric field shear. Neoclassical heat transport for thermals should be retained, also. Combining ion temperature gradient profile evolution, including turbulent and neoclassical transport and a heating power source, using radial force balance for mean $\langle E_r \rangle$, and including a realistic model of the profile-dependent drift mode growth rate will bring us to a 1D counterpart of the model of Ref. [54]. Here, f will no longer be a fixed parameter, but rather a quantity varying in radius and evolving in time, i.e., $f = f(r,t)$. The profile of f is obviously crucial, both to saturation levels and transport, and to the triggering, propagation and extent of any ITB. The spatiotemporal evolution of f will feed through the nonlinear dynamics, via dependence of coupling coefficients on dilution. It is not hard to see that this system can exhibit at least two regimes of enhanced confinement. These are:

a) at modest heat input, a regime of dilution enhanced zonal flow activity with improved confinement but still with finite drift wave fluctuations. Note that the latter are required to support the zonal flow.

b) at higher input power, a strong ITB state, with transport reduced close to or to neoclassical levels, a strong mean E×B shear, and little or no surviving zonal flow activity. Note that dilution would serve to reduce the power threshold to access this state, as compared to the level required with no dilution. The ITB state would, of course, be hysteretic. This may be exploited to expand the regime of enhanced confinement. An investigation of the scenario proposed above is the logical next step in our study of the dilution model.

Finally, it should be noted that the use of the dilution factor f is a crude surrogate for the evolution of the energetic particle (EP) distribution. For higher powers, the EPs can no longer be treated as passive. Instead, the EPs will unleash the beloved animalia of AEs and related EP modes. The EP distribution will then evolve *dynamically*, and the AEs will drive phase space structures and zonal modes. AE transport will result, and cross-scale coupling can be expected to occur between high-frequency AEs, mid-frequency drift waves, and low-frequency nonlinear structures and zonal modes. The theoretical description of this system is a very challenging problem in multi-scale interaction which will require significant future effort. Further discussion is not possible at this time.

Acknowledgment

The authors thank A. Bierwage, L. Chen, M.J. Choi, X.D. Du, J. Garcia, N.N. Gorelenkov, Z.B. Guo, H. Han, W.W. Heidbrink, A. Ishizawa, J. Kang, D.U. Kim, S.K. Kim, J.-M. Kwon, Z. Lin, P. Liu, Y.-S. Na, J.-K. Park, S.J. Park, G.E. Ronimo, C. Sung, J.P. Xi, Q. Yan, and S.M. Yang for helpful discussions. This research was supported by National R&D Program through the National Research Foundation of Korea(NRF) funded by Ministry of Science and ICT(NRF-2021M1A7A4091135, 2021M3F7A1084418, 2023R1A2C100773511), Basic Science Research Program through the National Research Foundation of Korea(NRF) funded by the Ministry of Education(2022R1I1A1A01072713), and U.S. Department of Energy under Award Number DE-FG02-04ER54738.

Appendix A

The response of wave action density to δu_{E} is given by Eqs. (12) and (13).

$$\delta N_q = iqk_x \delta u_{\mathrm{E},q} \frac{\partial \langle N \rangle}{\partial k_x} \tag{56}$$

$$R_q = (-i\Omega + iqv_{gx} + \Lambda)^{-1}. \tag{57}$$

Hereafter $\Lambda = |\gamma_q|$ as a convenient, calculable surrogate for decorrelation rate. Note then:

$$R_q = \frac{i}{\Omega - qv_{gx} + i|\gamma_q|}. \tag{58}$$

Then, proceeding as in the familiar, related case of the 1D Vlasov response [13],

$$R_q \sim \frac{1}{|\gamma_q|}, \quad \text{for} \quad \Omega \approx qv_{gx}, \tag{59}$$

and

$$R_q \sim \frac{1}{\Omega - qv_{gx}}, \quad \text{for} \quad |\Omega - qv_{gx}| > |\gamma_q|. \tag{60}$$

The first case occurs for resonance between the modulation field (zonal flow) and the drift wave packet and hence is referred to as the 'resonant' limit. It corresponds to 'strong turbulence' since the correlation time of δN and δu_{E} is ultimately set by $|\gamma_q|^{-1}$, which is long and which represents the decorrelation rate.

The second case occurs when $|\Omega - qv_{gx}|$ is finite and indeed $> |\gamma_q|$. In this case, the modulator field (zonal flow) and the drift wave packet are not resonant, so the limit is called 'non-resonant'. This corresponds to 'weak turbulence' since the correlation time of δN and δu_{E} is shorter, so interaction is weaker.

Strong turbulence is frequently observed at the edge, where fluctuation levels are larger. Weak turbulence is thought to occur in the core, where levels are usually lower.

Appendix B

The response operator for $R_{\mathbf{k}}$ for drift wave turbulence is given by

$$R_{\mathbf{k}} = \frac{\Delta\omega_{\mathbf{k}}}{(\omega_{\mathbf{k}} - k_y u_{\mathrm{ZF}})^2 + \Delta\omega_{\mathbf{k}}^2}. \tag{61}$$

For $\Delta\omega_{\mathbf{k}} > \Delta\omega (\sim 1/\tau_{\mathrm{ac}})$, we have "strong turbulence". In the case where $\omega_{\mathbf{k}} \sim k_y u_{\mathrm{ZF}}$,

$$R_{\mathbf{k}} \sim \frac{1}{\Delta\omega_{\mathbf{k}}}, \tag{62}$$

the *resonant*, strong turbulence response, giving Eq. (55c). For $\Delta\omega_{\mathbf{k}} < \Delta\omega$,

$$R_{\mathbf{k}} \approx \pi\delta(\omega_{\mathbf{k}} - k_y u_{\mathrm{ZF}}), \tag{63}$$

leading to Eq. (55d). This is the resonant, weak turbulence response, familiar from quasilinear theory. Note both cases are resonant. What differs is the relative size of the spectral width $\Delta\omega$ and the linewidth $\Delta\omega_{\mathbf{k}}$.

References

[1] W. Horton, *Rev. Mod. Phys.* **71**, 735 (1999)
[2] L. Chen and F. Zonca, *Rev. Mod. Phys.* **88**, 015008 (2016)
[3] A. Di Siena, A.B. Navarro and F. Jenko, *Phys. Rev. Lett.* **125**, 105002 (2020)
[4] N.N. Gorelenkov and V.N. Duarte, *Phys. Lett. A* **386**, 126944 (2021)
[5] A. Biancalani *et al.*, *Plasma Phys. Control. Fusion* **63**, 065009 (2021)
[6] A. Ishizawa *et al.*, *Nucl. Fusion* **61**, 114002 (2021)
[7] P. Liu *et al.*, *Phys. Rev. Lett.* **128**, 185001 (2022)
[8] S. Mazzi *et al.*, *Nat. Phys.* **18**, 776 (2022)
[9] A. Mishchenko *et al.*, *Plasma Phys. Control. Fusion* **64**, 104009 (2022)
[10] P.H. Diamond *et al.*, *Plasma Physics and Controlled Nuclear Fusion Research* (IAEA, Vienna) IAEA-CN-69/TH3/1 (1998)
[11] L. Chen, Z. Lin and R. White, *Phys. Plasmas* **7**, 3129 (2000)
[12] P.H. Diamond *et al.*, *Nucl. Fusion* **41**, 1067 (2001)
[13] P.H. Diamond *et al.*, *Plasma Phys. Control. Fusion* **47**, R35 (2005)
[14] L. Chen and F. Zonca, *Phys. Rev. Lett.* **109**, 145002 (2012)
[15] Z. Qiu, L. Chen and F. Zonca, *Phys. Plasmas* **23**, 090702 (2016)
[16] H. Han *et al.*, *Nature* **609**, 269 (2022)
[17] T.S. Hahm *et al.*, *Phys. Plasmas* **30**, 072501 (2023)
[18] T.S. Hahm *et al.*, *Plamsa Phys. Control. Fusion* **42**, A205 (2000)
[19] A. Fujisawa *et al.*, *Phys. Rev. Lett.* **93**, 165002 (2004)
[20] D.K. Gupta *et al.*, *Phys. Rev. Lett.* **97**, 12502 (2006)
[21] N. Winsor, J.L. Johnson and J.M. Dawson, *Phys. Fluids* **11**, 2448 (1968)
[22] T.S. Hahm *et al.*, *Phys. Plasmas* **6**, 922 (1999)
[23] G.Y. Fu, *Phys. Rev. Lett.* **101**, 185002 (2008)
[24] A.I. Smolyakov and P.H. Diamond, *Phys. Plasmas* **6**, 4410 (1999)
[25] M.A. Malkov and P.H. Diamond, *Phys. Plasmas* **8**, 3996 (2001)
[26] P.H. Diamond *et al.*, *Phys. Plasmas* **15**, 012303 (2008)
[27] T.H. Stix, *Waves in Plasmas* (AIP Publishing LLC. 1992)
[28] R. Balescu, *Aspects of Anomalous Transport in Plasmas* (IOP Publishing Ltd. 2005)
[29] G.I. Taylor, *Proc. R. Soc. Lond. A* **151**, 421 (1935)
[30] P.H. Diamond *et al.*, *Plasma Phys. Control. Fusion* **50**, 124018 (2008)
[31] S.M. Yang *et al*, *Phys. Plasmas* **25**, 122305 (2018)
[32] M.S. Hussein, W. Guo and L. Wang, *Plasma Phys. Control. Fusion* **63**, 075010 (2021)
[33] A. Di Siena *et al.*, *J. Plasma Phys.* **87**, 555870201 (2021)
[34] A. Di Siena *et al.*, *Phys. Rev. Lett.* **127**, 025002 (2021)
[35] D. Kim *et al.*, *Nucl. Fusion* **63**, 124001 (2023)
[36] T.S. Hahm and W.M. Tang, *Phys. Fliuds B* **1**, 1185 (1989)
[37] H. Du *et al.*, *Phys. Plasmas* **24**, 122501 (2017)
[38] M.N. Rosenbluth *et al.*, *Plasma Physics and Controlled Nuclear Fusion* (IAEA, Vienna), Vol. I, p. 495 (1971)
[39] F.L. Hinton and M.N. Rosenbluth, *Plasma Phys. Control. Fusion* **41**, A653 (1999)

[40] A. Hasegawa and K. Mima, *Phys. Fluids* **21**, 87 (1978)
[41] P.H. Diamond and M.N. Rosenbluth, *Phys. Fluids* **24**, 1641 (1981)
[42] R.J. Hawryluk, *Rev. Mod. Phys.* **70**, 537 (1998)
[43] R.V. Budny and JET Contributors, *Nucl. Fusion* **58**, 096011 (2018)
[44] Y. Koide *et al.*, *Phys. Rev. Lett.* **72**, 3662 (1994)
[45] Y. Kamada, *Plasma Phys. Control. Fusion* **42**, A65 (2000)
[46] M.J. Choi *et al.*, *Nat. Commun.* **12**, 375 (2021)
[47] G.R. McKee *et al.*, *Phys. Plasmas* **10**, 1712 (2003)
[48] F. Khabanov *et al.*, *presented at US Transport Task Force Meeting* (2023)
[49] T.S. Hahm and P.H. Diamond, *J. Korean Phys. Soc.* **73**, 747 (2018)
[50] G. Dif-Pradalier *et al.*, *Phys. Rev. E* **82**, 025401(R) (2010)
[51] P.B. Rhines, *J . Fluid Mech.* **69**, 417 (1975)
[52] A. Ashourvan and P.H. Diamond, *Phys. Rev. E* **94**, 051202(R) (2016)
[53] A. Ashourvan and P.H. Diamond, *Phys. Plasmas* **24**, 012305 (2017)
[54] E.-J. Kim and P.H. Diamond, *Phys. Rev. Lett.* **90**, 185006 (2003)